Annals of Biomedical Engineering, Vol. 48, No. 12, December 2020 *(© 2020)* pp. 2911–2923
https://doi.org/10.1007/s10439-020-02586-x

Original Article

Tricuspid Valve Annuloplasty Alters Leaflet Mechanics

MRUDANG MATHUR,[1] WILLIAM D. MEADOR,[2] TOMASZ JAZWIEC,[3,4] MARCIN MALINOWSKI,[4,5] TOMASZ A. TIMEK,[4] and MANUEL K. RAUSCH[6]

[1]Department of Mechanical Engineering, University of Texas at Austin, 204 E Dean Keeton Street, Austin, TX 78712, USA; [2]Department of Biomedical Engineering, University of Texas at Austin, 107 W Dean Keeton Street, Austin, TX 78712, USA; [3]Department of Cardiac, Vascular and Endovascular Surgery and Transplantology, Silesian Centre for Heart Diseases, Medical University of Silesia in Katowice, Zabrze, Poland; [4]Division of Cardiothoracic Surgery, Spectrum Health, Grand Rapids, MI 49503, USA; [5]Department of Cardiac Surgery, School of Medicine in Katowice, Medical University of Silesia, Katowice, Poland; and [6]Departments of Aerospace Engineering & Engineering Mechanics, Biomedical Engineering, University of Texas at Austin, 2617 Wichita Street, Austin, TX 78712, USA

(Received 15 February 2020; accepted 27 July 2020; published online 6 August 2020)

Associate Editor Elena S. Di Martino oversaw the review of this article.

Abstract—Tricuspid valve regurgitation is associated with significant morbidity and mortality. Its most common treatment option, tricuspid valve annuloplasty, is not optimally effective in the long-term. Toward identifying the causes for annuloplasty's ineffectiveness, we have previously investigated the technique's impact on the tricuspid annulus and the right ventricular epicardium. In our current work, we are extending our analysis to the anterior tricuspid valve leaflet. To this end, we adopted our previous strategy of performing DeVega suture annuloplasty as an experimental methodology that allows us to externally control the degree of cinching during annuloplasty. Thus, in ten sheep we successively cinched the annulus and quantified changes to leaflet motion, dynamics, and strain in the beating heart by combining sonomicrometry with our well-established mechanical framework. We found that successive cinching of the valve enforced earlier coaptation and thus reduced leaflet range of motion. Additionally, leaflet angular velocity during opening and closing decreased. Finally, we found that leaflet strains were also reduced. Specifically, radial and areal strains decreased as a function of annular cinching. Our findings are critical as they suggest that suture annuloplasty alters the mechanics of the tricuspid valve leaflets which may disrupt their resident cells' mechanobiological equilibrium. Long-term, such disruption may stimulate tissue maladaptation which could contribute to annuloplasty's sub-optimal effectiveness. Additionally, our data suggest that the extent to which annuloplasty alters leaflet mechanics can be controlled *via* degree of cinching. Hence, our data may provide direct surgical guidelines.

Address correspondence to Manuel K. Rausch, Departments of Aerospace Engineering & Engineering Mechanics, Biomedical Engineering, University of Texas at Austin, 2617 Wichita Street, Austin, TX 78712, USA. Electronic mail: manuel.rausch@utexas.edu

Keywords—Annulus, Functional regurgitation, Maladaptation, Growth and remodeling, DeVega.

INTRODUCTION

The tricuspid valve regulates blood flow from the right atrium into the right ventricle. During diastole, the transvalvular pressure gradient opens the valve and permits right ventricular filling. By contrast, a reverse pressure gradient during systole closes the tricuspid valve, which prevents retrograde blood flow.[25,33,54] In nearly 1.6 million patients in the US, tricuspid valve coaptation is insufficient, resulting in moderate to severe tricuspid valve leakage, or tricuspid valve regurgitation.[60] In most of these patients, tricuspid regurgitation is "functional" meaning that its origin is ostensibly extrinsic to the valve itself.[12] For example, in patients with left heart disease, mechanical and hemodynamic coupling between the ventricles results in right ventricular remodeling. Subsequently, right ventricular dilation and papillary muscle displacement increase the tricuspid valve orifice area and tether its leaflets, respectively. Similarly, in patients with pulmonary hypertension, right ventricular remodeling also results in annular dilation and leaflet tethering. In both presentations, increased orifice area and tethered leaflets then inhibit leaflet coaptation and induce functional tricuspid regurgitation.[59] Clinically, functional tricuspid regurgitation is addressed by prosthetic ring annuloplasty or DeVega suture annuloplasty.[30]

During these invasive surgical repairs, the tricuspid valve annulus is cinched to reduce the valve's orifice area and to approximate the leaflets. Together, orifice area reduction and leaflet approximation improve valve closure and reduce regurgitation. However, these procedures are often sub-optimally effective in the long run with only 22% of patients being free of regurgitation five years post-operatively.[36]

The exact causes for the aforementioned repair failures are currently unknown. However, it is possible that continued remodeling of the right ventricle further displaces the papillary muscles and worsens leaflet tethering despite repair on the annular level.[36] Alternatively or additionally, it is possible that tricuspid leaflet maladaptation actively contributes to repair failure.[42] On the left side of the heart, patients with heart failure present with thickened and stiffened mitral leaflets, which ostensibly contributes to mitral valve failure in those patients.[13,14] Similarly, studies in large animals with leaflet tethering and/or left ventricular ischemia have demonstrated mitral valve leaflet maladaptation.[10] Interestingly, mitral valve annuloplasty itself has also been shown to elicit a maladaptive tissue response. Sielicka *et al.* have shown that implantation of mitral valve annuloplasty devices in pigs with ischemic mitral regurgitation elevated levels of collagen expression.[53] Moreover, mitral valve leaflets from those animals also exhibited stiffer behavior than those from control animals. Therefore, in the mitral valve, surgical repair *via* annuloplasty may further contribute to the already present disease-induced leaflet maladaptation and thus risk repair efficacy. Either way, mitral leaflets maladapt, at least in part, due to changes in their mechanical environment during disease or in response to annuloplasty.[61] While there is currently no evidence for similar maladaptive mechanisms to disease and repair in the tricuspid valve, given similarities in structure, function, and resident cell phenotypes between the mitral and the tricuspid valve, it is likely that tricuspid valve leaflets show similar maladaptation in response to disease and/or repair.

The investigation of similar mechanisms in the tricuspid valve must begin with characterising its anatomy,[16,26] microstructure[35,50,57] and structure-function relationship[3,38,58] and identifying changes in its *in-vivo* mechanics. In fact, we have recently shown that suture annuloplasty in animals with biventricular heart failure-induced functional tricuspid regurgitation present with altered right ventricular mechanics and valvular competence.[18] In our current work, we investigate whether tricuspid annuloplasty alters the mechanics of the tricuspid valve leaflets. Specifically, we will investigate the anterior leaflet's *in-vivo* mechanics as a function of degree of annular cinching. To this end, we use DeVega suture annuloplasty as an experimental methodology that allows us to externally control the degree of cinching. Thus, we will take a step toward uncovering whether tricuspid valve repair may inadvertently contribute to tricuspid valve disease and thus, at least in part, explain the high rate of repair failure. To this end, we utilize our previously established kinematic framework in combination with sonomicrometry in sheep.

METHODS

Animal Model

We performed all animal and experimental procedures with strict adherence to the Principles of Laboratory Animal Care, formulated by the National Society for Medical Research, and the Guide for Care and Use of Laboratory Animals prepared by the National Academy of Science and published by the National Institutes of Health. This protocol was also approved by our local Institutional Animal Care and Use Committee (Spectrum Health IACUC #:18-01).

We have previously provided detailed descriptions of all surgical procedures.[32] In short, we used propofol to intravenously anesthetize ten male Dorset sheep (60 ± 3 kg) before intubating and placing the animals on mechanical ventilation. We then performed a median sternotomy to expose the heart and prepared the animals for cardiopulmonary bypass. Upon initiating cardiopulmonary bypass and on the beating heart, we performed an atriotomy and placed the DeVega annuloplasty suture around the tricuspid annulus, as described previously in Ref. 31. We performed the DeVega procedure with two 2–0 polypropylene sutures in two layers around the tricuspid valve orifice and anchored the sutures with pledgets at the antero-septal commissure and the mid-septal annulus. To control the degree of cinching, we subsequently externalized the annuloplasty suture through the antero-posterior commissure to a tourniquet. We then implanted six 2 mm sonomicrometry crystals (Sonometrics Corp, London, Ontario, Canada) around the tricuspid annulus with one crystal at the antero-septal, antero-posterior, and posterio-septal commissures and each of the three mid-commissural points, creating six annular regions, Fig. 1a. Next, we sutured four 1mm sonomicrometry crystals in a diamond pattern on the anterior tricuspid valve leaflet and externalized the crystal wires for data acquisition through an atriotomy, see Fig. 1a. Additionally, we recorded hemodynamics with pressure transducers (PA4.5-X6; Konigsberg Instruments, Inc, Pasadena, CA) placed in the left ventricle, right ventricle, and right atrium. After weaning the animals off cardiopulmonary by-

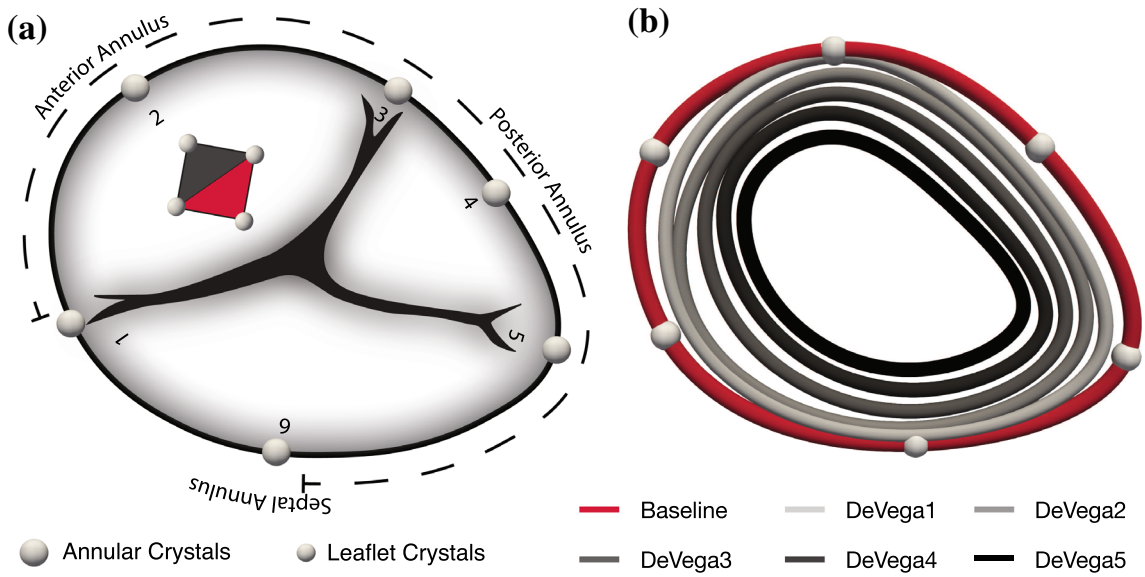

FIGURE 1. (a) Depiction of the tricuspid valve with annular sonomicrometry crystals (1–6, 2 mm diameter) and the approximate location of the DeVega suture annuloplasty (dashed line). The diamond on the anterior leaflet depicts the area between leaflet sonomicrometry crystals (1 mm diameter). The grey area denotes the "belly" region, while the red area represents the "free-edge" region. (b) Annular geometry based on a cubic spline fit to sonomicrometry crystals 1–6 at Baseline and each DeVega suture annuloplasty cinching step. With permission reproduced from Ref. 31.

pass, we allowed the animals to recover for 30 minutes under anesthesia to achieve stable hemodynamics. Note, during these experiments we collected data on the tricuspid annulus, which we previously reported,[31] as well as for our current work.

Data Acquisition

Once the animals stabilized we recorded sonomicrometry data using SonoSoft (Sonometrics Corporation, London, Ontario, Canada), hemodynamic data, and echocardiographic data for three consecutive cardiac cycles to establish a baseline.[19] Next, we cinched the sutures by approximately 2 cm (DeVega1), allowed the hemodynamics to stabilize again, and recorded additional data. We repeated this cinching process four more times (DeVega2-5), thereby reducing annular size at each stage, see Fig. 1b. After completing the experiments, we euthanized the animals by administering sodium pentothal and potassium chloride. Finally, we dissected the hearts and verified proper crystal positioning. Also note, small posterior and septal leaflets render crystal data less reliable than for the anterior leaflet. Therefore, we chose to report data only on the anterior leaflet in our current work.

Annular Reconstruction

To recreate smooth annuli from discrete data points we used Matlab (MathWorks, Natick, MA) to fit a cubic spline, in a least-squares sense, to the triangulated positions of the six annular sonomicrometry crystals. We have previously described this procedure in detail and refer the reader to our work on both the mitral[44,48] and the tricuspid annulus.[45,46]

Leaflet Motion

To examine the motion of the anterior tricuspid valve leaflet we considered a radial line passing through the leaflet center. To this end, we fit a cubic spline through the mid-annular segment crystal, the mid-belly crystal, and the free-edge crystal, as well as a fourth crystal position, which we created by calculating the mean position of the two lateral crystals. Additionally, we fit a least-squares plane to the annular crystals at each time point. To quantify the opening and closing angles, we measured the angle between the cubic spline and this plane throughout the cardiac cycle with the annular plane representing 0°. Furthermore, we used these data to determine angular velocities using a finite-difference scheme.

Leaflet Strain Computation

To quantify strains in the anterior tricuspid valve leaflet during the DeVega suture annuloplasty procedure we used an approach previously described in.[43,47] To this end, we interpolated the two triangular elements *via* linear shape functions in terms of the local curvilinear coordinates θ^{α}, where $\alpha = 1, 2$ as in Eq. (2). Here, we chose end-diastole to be the reference con-

figuration, whose interpolated coordinates are represented by $\mathbf{X}(\theta^1, \theta^2)$, with $\mathbf{x}(\theta^1, \theta^2)$ being the interpolated coordinates in the spatial configuration which varied throughout the cardiac cycle and between DeVega cinching stages. On the other hand, $N_i(\theta^1, \theta^2)$ are linear shape functions used to interpolate the crystal coordinates in the reference and spatial configurations, $\mathbf{X}_i$ and $\mathbf{x}_i$, respectively,

$$\mathbf{X}(\theta^1, \theta^2) = \sum_{i=1}^{3} N_i(\theta^1, \theta^2)\mathbf{X}_i \tag{1}$$

and

$$\mathbf{x}(\theta^1, \theta^2) = \sum_{i=1}^{3} N_i(\theta^1, \theta^2)\mathbf{x}_i. \tag{2}$$

We used the partial derivatives of the shape functions delineated above to compute the covariant basis vectors in the reference and spatial configurations,

$$\mathbf{G}_\alpha(\theta^1, \theta^2) = \sum_{i=1}^{3} \partial N_i / \partial \theta^\alpha \mathbf{X}_i \tag{3}$$

and

$$\mathbf{g}_\alpha(\theta^1, \theta^2) = \sum_{i=1}^{3} \partial N_i / \partial \theta^\alpha \mathbf{x}_i, \tag{4}$$

while we determined the contravariant counterparts to the above bases *via* the covariant surface metric in the reference configuration, $G_{\alpha\beta} = G_\alpha \cdot G_\beta$, i.e,

$$\mathbf{G}^\alpha = G^{\alpha\beta}\mathbf{G}_\beta, \text{ where } G^{\alpha\beta} = G_{\alpha\beta}^{-1}, \text{ with } \alpha, \beta = 1, 2, \tag{5}$$

and *via* the covariant surface metric in the current configuration $g_{\alpha\beta} = g_\alpha \cdot g_\beta$, i.e,

$$\mathbf{g}^\alpha = g^{\alpha\beta}\mathbf{g}_\beta, \text{ where } g^{\alpha\beta} = g_{\alpha\beta}^{-1}. \tag{6}$$

Furthermore, we calculated the Green–Lagrange strain tensor as,

$$\mathbf{E} = E_{\alpha\beta}\mathbf{G}^\alpha \otimes \mathbf{G}^\alpha, \text{ where } E_{\alpha\beta} = \frac{1}{2}[g_{\alpha\beta} - G_{\alpha\beta}]. \tag{7}$$

We projected the resulting full strain tensor onto the circumferential and radial directions $\mathbf{n}_c$ and $\mathbf{n}_r$, respectively, to derive the circumferential strain E_c and the radial strain E_r for each triangular element, see Eq. 8. Detailed descriptions of this procedure are provided in our previous work.[6,7]

$$E_c = \mathbf{n}_c \cdot \mathbf{E}\mathbf{n}_c, \text{ and } E_r = \mathbf{n}_r \cdot \mathbf{E}\mathbf{n}_r \tag{8}$$

Temporal Averaging

As heart rates varied between animals we aligned temporal evolutions of all quantities of interest by first dividing them into four distinct segments: end-diastole to end-isovolumic contraction, end-isovolumic contraction to end-systole, end-systole to end-isovolumic relaxation, and end-isovolumic contraction to end-diastole of the next cardiac cycle. Next, we normalized the duration of each segment, linearly interpolated crystal locations throughout each segment, averaged those segments between animals, and re-assembled the average segments into an average temporal curve. We used this same procedure on vectorial quantities, such as displacement, in that we treated each coordinate as an independent scalar.

Statistics

Before comparing differences in opening angle, angular velocity, and strain, we used the Shapiro-Wilk's test to determine whether data were normally distributed. If normal, we used the paired Student's *t* test to compare opening angles and angular velocity between DeVega steps and DeVega steps and baseline. If not, we used the Wilcoxon signed-rank test in lieu of the paired Student's *t* test. Similarly, if normal, we used a one sample Student's *t* test to compare strains for each DeVega step against a mean of zero. If not, we used again the Wilcoxon signed-rank test in lieu of the Student's *t* test. We performed all statistical analyses in Matlab R2019a. We reported all data as mean ± standard error unless mentioned otherwise. For all tests, we considered a p-value less than 0.05 as statistically significant.

RESULTS

All sheep recovered well from surgery and we successfully collected sonomicrometry data for all ten animals, see Table 1 for a summary of hemodynamic data.

Based on the sonomicrometry analysis and averaging technique described in Sections "Leaflet Strain Computation" and "Temporal Averaging", we captured the closing mechanics of the average anterior leaflet midline between end-diastole and end-systole for baseline and each DeVega step (Fig. 2). Although the end-diastolic position of the leaflet did not significantly change with each cinching step, the end-systolic position of the leaflets appeared to change with increased cinching (Fig. 2a. Note, in this figure we shifted the midline crystals of the anterior leaflet to coincide for baseline and each DeVega step for direct

TABLE 1. Hemodynamics for baseline (BSL) and each DeVega (DV) cinching step.

			BSL	DV1	DV2	DV3	DV4	DV5
HR	(bpm)	Mean	115.0	112.6	112.8	109.7	110.6	111.7
		STD	5.1	6.3	6.3	8.4	7.4	7.2
LVP_{ES}	(mmHg)	Mean	60.91	63.44	59.69	57.72	55.10	53.06
		STD	10.42	11.97	16.64	18.55	17.29	15.27
LVP_{ED}	(mmHg)	Mean	12.61	12.29	10.33	9.55	9.77	10.18
		STD	5.06	5.64	6.24	5.20	5.44	4.87
RVP_{ES}	(mmHg)	Mean	20.27	22.00	25.74	25.29	23.29	22.88
		STD	4.65	3.71	5.96	8.27	5.86	6.89
RVP_{ED}	(mmHg)	Mean	8.12	8.55	8.88	10.48	11.13	11.80
		STD	3.27	2.84	2.12	2.77	3.77	4.01
RAP_{ES}	(mmHg)	Mean	13.10	13.13	12.96	13.66	13.95	14.37
		STD	3.35	3.01	2.27	2.46	3.02	2.73
RAP_{ED}	(mmHg)	Mean	4.68	4.83	5.51	5.13	4.37	4.39
		STD	2.84	3.25	3.53	2.98	3.51	3.99
TVP	(mmHg)	Mean	0.98	1.08	1.40	1.70	2.34	**3.34**
		STD	0.36	0.50	0.62	0.84	1.52	**1.78**

Heart rate (HR), left ventricular pressure (LVP), right ventricular pressure (RVP), right atrial pressure (RAP), echo-derived transvalvular gradient (TVP), end-diastole (ED), end-systole (ES). Bold faced quantities were significantly different from baseline values, i.e. $p < 0.05$.

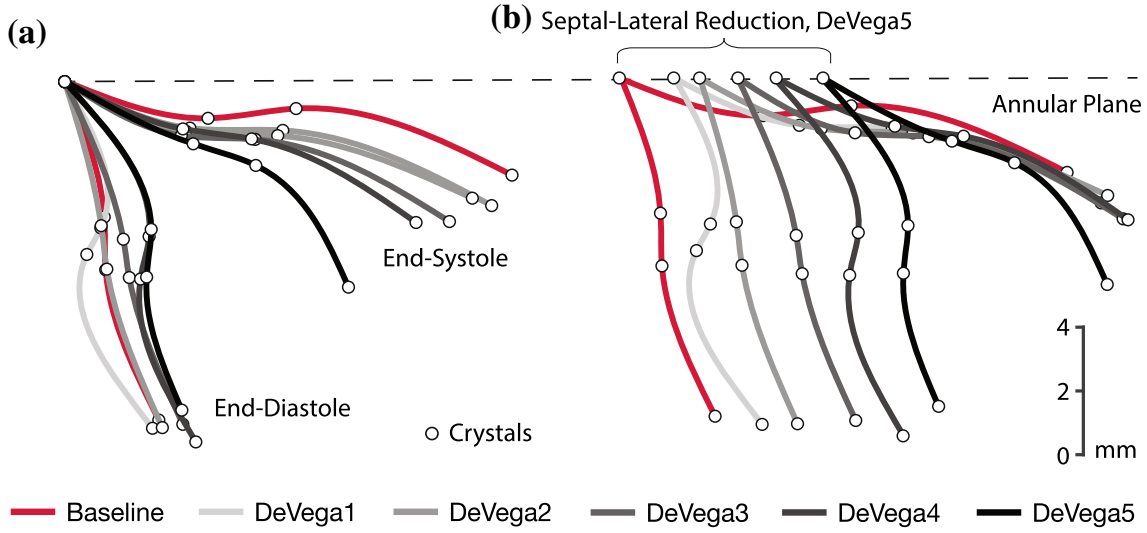

FIGURE 2. DeVega suture annuloplasty altered the closing mechanics of the anterior leaflet. (a) For direct comparison between DeVega steps, the annular insertion point of the anterior leaflet midlines were shifted to align between baseline and each DeVega step. The midlines show that, while the end-diastolic position did not significantly differ, the end-systolic positions were affected by the DeVega suture annuloplasty. (b) Depiction of the same geometries as in (a), while also accounting for the shift of the annular crystal during cinching.

comparison). Specifically, with increased cinching the anterior leaflet increased its end-systolic angle relative to the annular plane. This change was likely due to the valve's septal-lateral reduction and, thus, altered proximity between the anterior leaflet and its opposing leaflets. In other words, the leaflets coapted after traversing a smaller angle with increased cinching. This septal-lateral reduction of the annular insertion point of the anterior leaflet following annular cinching is visualized in Fig. 2b. Note that the free-edge sonomicrometry crystal in systole remained in a similar position independent of degree of cinching, highlighting a consistent site of leaflet coaptation despite alterations in annular size.

Using the same sonomicrometry crystal positions, we calculated temporal evolutions and peak values of the opening/closing angle and velocities throughout the cardiac cycle for baseline and each DeVega step (Fig. 3). As expected, the anterior leaflet underwent significant angular changes throughout the cardiac cycle. Qualitatively, for baseline and all DeVega steps the leaflet began in an open position at end-diastole

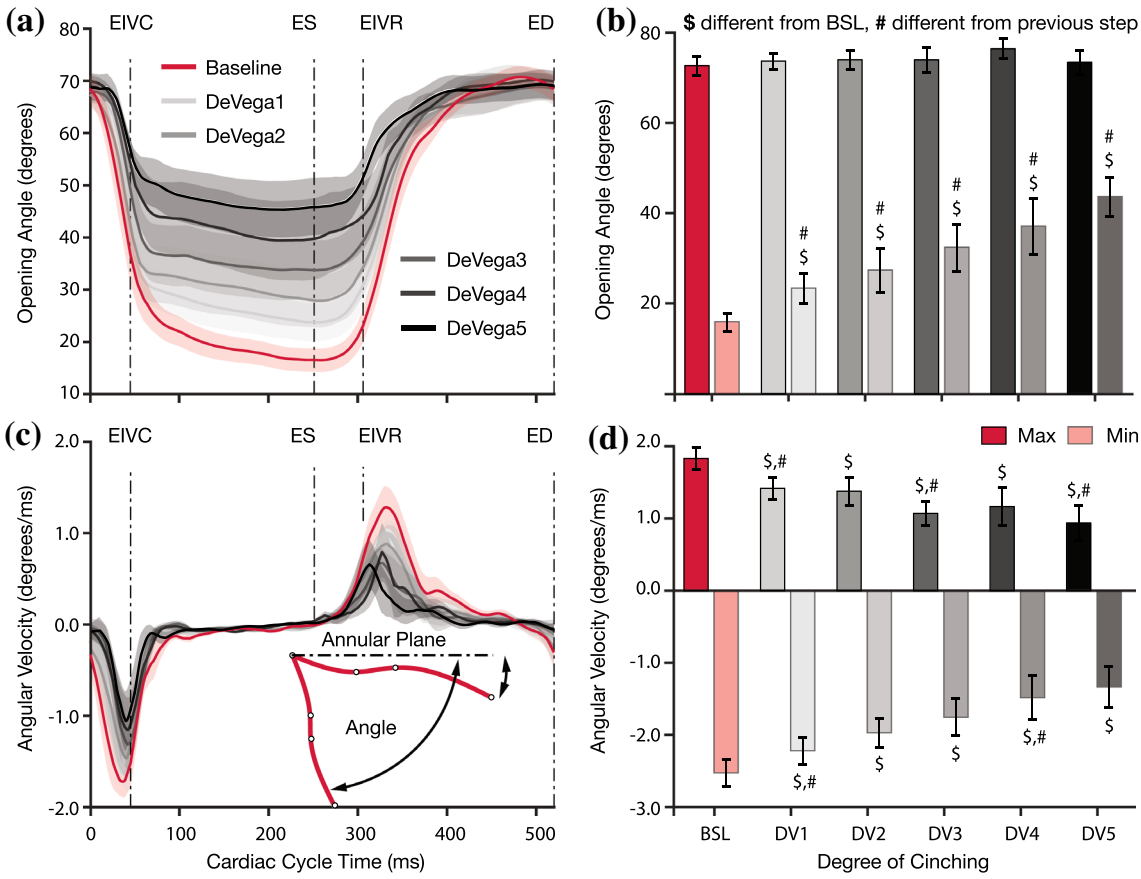

FIGURE 3. DeVega suture annuloplasty altered leaflet opening/closing angle and velocity. (a, b) Successive annular cinching *via* DeVega suture annuloplasty (DV) reduced the leaflet range of motion during the cardiac cycle. Specifically, DeVega suture annuloplasty increased the maximum opening angle (measured against the annular plane), which, in combination with an unaffected minimum angle, led to a reduction in annular motion. (c, d) Successive annular cinching steps (DV1-5), reduced the leaflet opening/closing velocity profile. Specifically, both maximum and minimum angular velocities decreased significantly for all cinching steps (relative to baseline (BSL)). End-Diastole (ED), End-Isovolumic Contraction (EIVC), End-Systole (ES), End-Isovolumic Relaxation (EIVR). Significant differences between current step and baseline are indicated by $, and those between current step and previous step by #. All data shown as mean ± standard error.

before an accelerated closing during isovolumic contraction, a period of little change during most of systole, and a rapid opening during isovolumic relaxation. Quantitatively, we found that all DeVega steps maintained similar end-diastolic angles relative to the annular plane of approximately 70° (Fig. 3a). During systole, however, DeVega suture annuloplasty greatly reduced the anterior leaflet range of motion. Specifically, at end-isovolumic contraction, end-systole and end-isovolumic relaxation, we observed increasing angles relative to the annular plane for larger cinching steps. The maximum and minimum angles for all groups were achieved near end-diastole and end-systole, respectively. We also quantified minimum and maximum angles throughout the cardiac cycle; in Fig. 3b the minimum and maximum opening angles are summarized for each group. Consistently, we found that the maximum angle during diastole remained mostly unchanged with cinching, while the minimum angle during systole significantly increased with each successive cinching step.

Again qualitatively, the angular velocity profiles looked identical between baseline and all DeVega steps. For example, the maximum and minimum angular velocities occurred at the same cardiac time point for baseline and DeVega steps (approximately end-isovolumic relaxation and end-isovolumic contraction, respectively). Quantitatively, we found that successive annular cinching reduced the magnitude of leaflet angular velocity (Fig. 3c). Consistently, we found significant reductions in the magnitude of maximum and minimum angular velocities with successive annular cinching (Fig. 3d). Overall, DeVega suture annuloplasty reduced the range of motion and the angular velocity of the anterior leaflet.

From the belly region sonomicrometry crystals, we also calculated circumferential, radial, and areal strains throughout the cardiac cycle (Fig. 4). We found

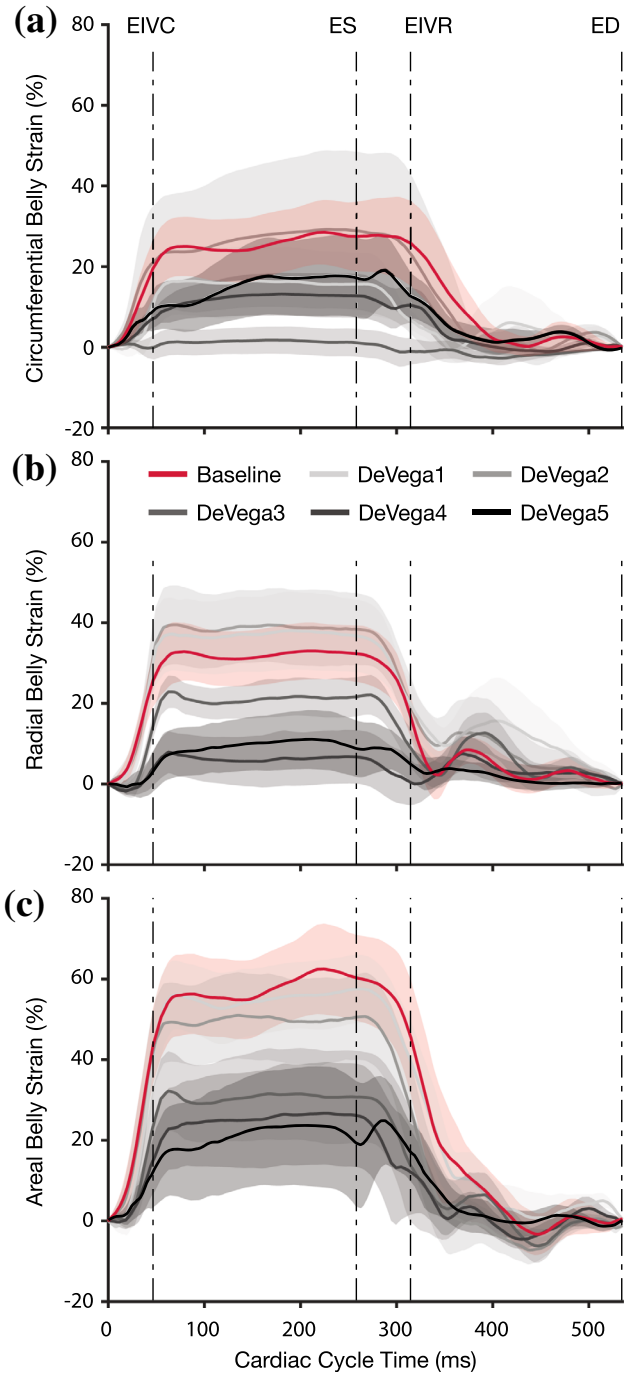

FIGURE 4. DeVega suture annuloplasty altered strain profiles throughout the cardiac cycle. (a) Circumferential leaflet belly strains, while remaining qualitatively similar to baseline, were successively reduced through annular cinching. (b) Similarly, radial leaflet belly strains, while remaining qualitatively similar to baseline, were altered through annular cinching (albeit less predictably than circumferential strains and to a larger degree). (c) Finally, areal leaflet belly strains were successively and significantly reduced through annular cinching. End-Diastole (ED), End-Isovolumic Contraction (EIVC), End-Systole (ES), End-Isovolumic Relaxation (EIVR). All data shown as mean ± standard error.

that annular cinching resulted in qualitatively similar temporal evolutions of circumferential strains but with successively reduced magnitude (Fig. 4a). For radial strains, we observed less predictable changes following annular cinching. Initial cinching (i.e., DeVega1) resulted in similar radial strains to baseline, but each successive reduction thereafter decreased radial strains to a large degree (Fig. 4b). Most consistently, we observed a successive decrease in areal strains with each cinching step. In initial cinching steps (i.e., DeVega1 and 2), we observed large changes between cinching steps, which reduced at late cinching steps (i.e., DeVega3, 4, and 5, Fig. 4c). To simplify the observation to only a single time point in the cardiac cycle, refer to Fig. 5a for the belly circumferential, radial, and areal strains at end-systole. Relative to baseline, annular cinching did not result in significantly altered circumferential strains. However, areal and radial strains were significantly reduced from baseline values (which are equal to zero) in DeVega3, 4, and 5 (Fig. 5a). Therefore, it is likely that radial strain reduction drove the reduction in areal strains during DeVega suture annuloplasty. We also investigated anterior leaflet areal belly strain at end-systole as a function of anterior annulus reduction (acquired from least-squares cubic spline fits to the annular sonomicrometry crystals) (Fig. 5b). Interestingly, we found that the end-systole areal strain reduction scaled approximately (and on average) linearly with anterior annulus reduction. Overall, we found that DeVega suture annuloplasty altered the belly strain profile throughout the cardiac cycle, most notably reducing radial and areal strains for larger cinching steps.

Table 2 summarizes radial, circumferential, and areal strains for both the belly and free-edge region. Data on the belly strain is identical to that presented in Fig. 4a. Note that none of the differences between the free-edge strains reached statistical significance, possibly implying that DeVega suture annuloplasty primarily altered belly strains but not free-edge strains.

DISCUSSION

Annuloplasty is a common surgical technique that reduces annular orifice area to mitigate leakage of the otherwise functional valve. Despite annuloplasty being a highly mechanical procedure, data on its mechanical effects on the tricuspid valve are sparse. In our previous work, we have investigated the effect of annuloplasty on annular mechanics in healthy sheep[28,31] and in an acute right heart failure model.[29] Additionally, we have reported on the effects of annuloplasty on the right ventricular epicardium in, again, healthy sheep[27] and sheep with tachycardia-induced biventricular heart

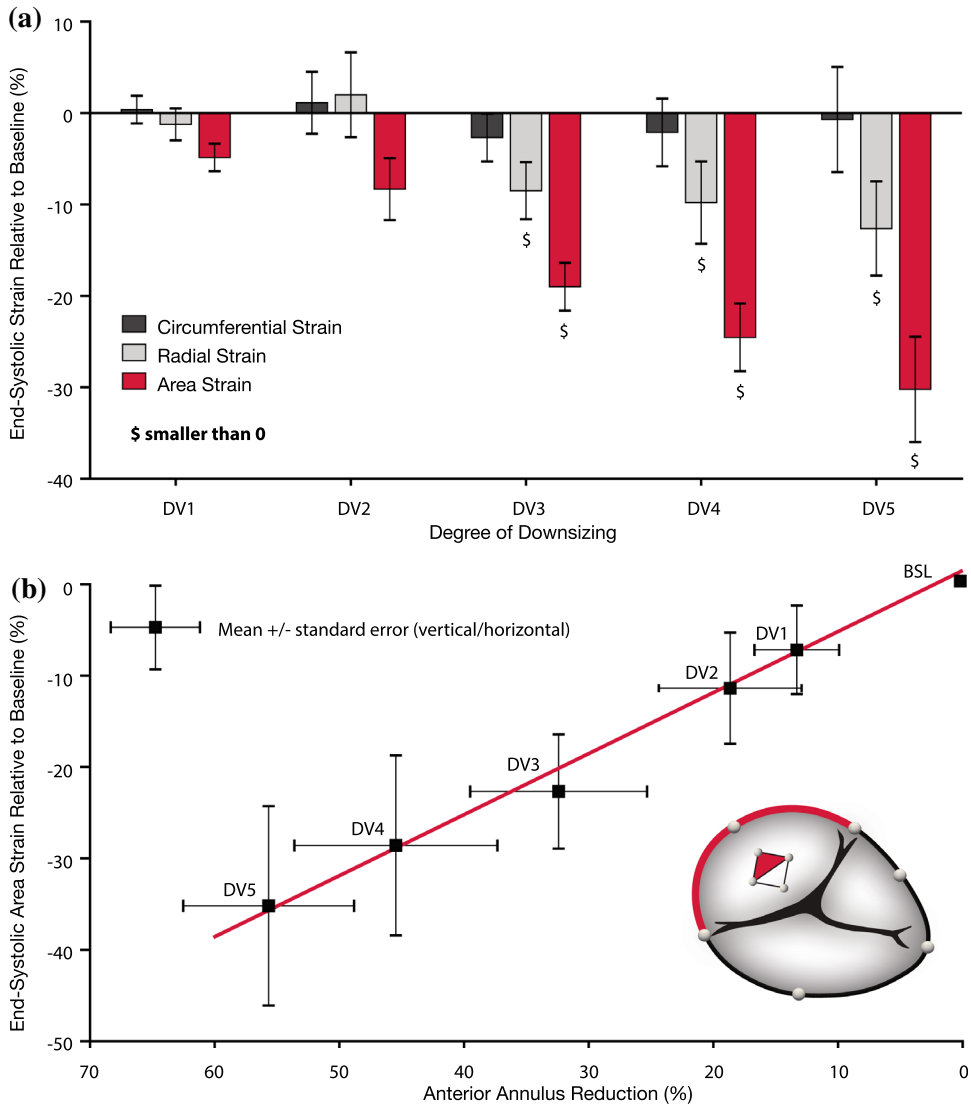

FIGURE 5. DeVega suture annuloplasty reduced end-systolic areal belly strain as a function of degree of annular cinching. (a) End-systolic areal and radial strain were reduced through annular cinching (statistically significantly starting with DeVega (DV) 3), while end-systolic circumferential strain appeared unaffected. (b) End-systolic areal belly strain decreased approximately linearly with anterior annulus reduction (relative to baseline (BSL)). Significant differences between current step and baseline are indicated by $. All data are shown as mean ± standard error. Note, an alternate version of this figure that shows raw data in form of a jitter plot can be found in the electronic supplement to this article.

failure.[18] No previous reports address the impact of annuloplasty on the leaflets themselves. Therefore, in our current study, we investigated how tricuspid valve annuloplasty alters anterior leaflet mechanics through the use of sonomicrometry in sheep. To this end, we implanted sonomicrometry crystals along the tricuspid annulus and in the belly and free-edge region of the anterior leaflet of these sheep. Before and after five consecutive cinching steps *via* externalized sutures, we successfully tracked and kinematically analyzed the positions of these crystals throughout the cardiac cycle.

By reporting on the leaflet position and range of motion after DeVega suture annuloplasty, we provided a quantitative picture of the mechanisms through which annuloplasty improves valvular function. We found that annuloplasty shifted the anterior leaflet position toward the septum at end-systole, while its end-diastolic position was unaffected. Earlier coaptation with the opposing leaflets during systole resulted in a smaller range of motion. Thus, in dilated valves annular cinching would decrease areal demands and improved the likelihood for coaptation. Interestingly, with less time to accelerate, peak angular velocities (during systole and diastole) also dropped.

In a single heartbeat, heart valve leaflets are subject to a number of deformation modes including bending,

TABLE 2. Circumferential (Circ.), radial (Rad.), and areal strains in the belly region and the free edge region of the anterior tricuspid valve leaflet.

			DV1		DV2		DV3		DV4		DV5	
			ED	ES	ED	ES	ED	ES	ED	ES	ED	ES
Circ. strain	Belly	Mean	2.45	0.37	1.03	1.12	1.86	− 2.68	2.90	− 2.13	2.77	− 0.71
		STD	5.22	4.76	10.32	10.72	8.88	8.28	9.43	11.72	8.97	18.20
	Free	Mean	7.36	− 2.19	5.72	− 0.74	3.54	− 4.25	4.92	− 4.32	6.50	6.51
		STD	13.06	5.82	12.25	6.67	14.13	8.27	17.22	8.77	18.33	29.34
Rad. strain	Belly	Mean	− 3.73	− 1.24	− 0.94	1.99	− 6.61	− **8.49**	− 0.24	− **9.80**	− 2.11	− **12.63**
		STD	13.14	5.51	10.01	14.68	11.12	**9.87**	21.56	**14.21**	22.90	**16.30**
	Free	Mean	8.56	− 1.91	20.27	19.63	16.43	13.20	21.51	7.64	29.31	1.35
		STD	32.32	13.02	42.67	46.12	44.59	59.06	47.96	40.47	67.99	38.92
Areal strain	Belly	Mean	− 3.89	− 4.86	− 2.36	− 8.33	− 8.15	− **19.00**	− 10.29	− **24.53**	− 11.15	− **30.22**
		STD	17.37	16.21	20.99	20.54	20.89	**21.98**	37.47	**32.03**	28.36	**36.12**
	Free	Mean	14.67	− 6.27	21.55	11.74	13.67	− 5.95	16.74	− 4.27	24.37	− 3.19
		STD	43.59	17.67	50.27	32.19	47.00	38.28	56.71	30.67	77.96	38.11

We calculated all strains relative to baseline at end-diastole (ED) and end-systole (ES) for each level of cinching, i.e. DeVega (DV) 1–5. Therefore, baseline strains are zero at both ED and ES. Bold-faced strains were statistically significant different from zero, i.e. $p < 0.05$.

tension, compression, and shear.[51] In the case of the tricuspid valve, these modes result from a complex set of loads due to the transvalvular pressure gradient, compressive forces due to the dynamically contracting annulus, chordal tethering forces, and shear stress due to blood flow.[21,22,23,55,63] Interestingly, we found that annuloplasty reduced anterior leaflet strain. It appears that the large decreases in areal strain in the belly of anterior leaflets was driven primarily by reductions in radial strain rather than changes in circumferential strain. It is possible that the decrease in radial strain was due to reduced chordal tethering—that is, with reduced range of motion, the leaflets coapted in a position more proximal to the papillary muscles, reducing the tethering forces and resultant radial strains. Another factor to consider is that anterior tricuspid valve leaflets are mechanically anisotropic, exhibiting stiffer circumferential behavior due to a mostly circumferential collagen orientation.[1,20,24,34,40] Therefore, changes in loading from annuloplasty may affect the directional strains of the tissue differently.

Changes in the mechanobiological equilibrium of soft tissues, such as tricuspid valve leaflet tissue, are known to drive compositional and configurational changes, e.g. growth and remodeling, to adapt to this altered environment.[2,15,17] In fact, multiple studies have shown that pathological mechanical stimuli in heart valve leaflets, at least in part, increase valvular interstitial cell activation and collagen turnover, which may result in maladaptive leaflet changes.[4,8,11,62] Therefore, we must consider that annuloplasty, by altering the mechanobiological equilibrium of the tissue (as shown in here), may elicit a biological response from these actively adapting leaflets.[53] Given the sparsity of data on tricuspid valve growth and remodeling, we can only hypothesize how changes induced *via* annuloplasty may affect the leaflets. For instance, it is possible that a decrease in strain may tilt the balance between synthesis and degradation toward the latter, resulting in increased enzymatic activity and decreased collagen synthesis, eventually rendering the tissue less stiff.[5] These effects may be directionally dependent, thus, altering not only the absolute stiffness, but also the tissue's anisotropy.[49] Therefore, it may be of interest in future studies to determine whether the altered leaflet mechanics following annuloplasty elicit a biological maladaptive response, and, if detrimental, to develop medical procedures which minimize mechanical changes to the native tissue environments.

It is also interesting to note that the atrioventricular heart valve annuli contract during systole, thus reducing annular orifice area as the valve closes. Our data show that reduction in orifice area reduces leaflet strain and thus stress. Therefore, our data indicate that annular contraction may not only increase leaflet area to orifice area ratio and thus aid valve competence, but also reduce leaflet strain and thus stress during systole. In other words, reduction of annular dynamics *via* rigid angioplasty devices may alter leaflet resident cell's mechanobiological equilibrium regardless of their size. Thus, even true-sized rigid devices may affect leaflet mechanobiology by altering the natural dynamics of leaflet.

While we used DeVega suture annuloplasty primarily as an experimental technique that allowed us to externally control degree of cinching, our data also reveal new information about the procedure itself. DeVega suture annuloplasty has been criticized for its inconsistent efficacy.[39] Mixed results were most likely

due to lack of concrete guidelines for surgeons.[52] Our study is useful clinically as it quantifies the degree to which DeVega suture annuloplasty alters leaflet position, dynamics, and deformation as a function of the degree of cinching. Additionally, our data is important for device annuloplasty. Specifically, our data may be useful as they provide a means to gauge the effect of cinching on the leaflets and may thus enable better informed surgical decisions. Furthermore, our study revealed an approximately linear relationship between annular reduction and areal strain of the leaflet. These data could be used to predict changes to the mechanobiological equilibrium of the leaflets, and thus, predict potential long-term effects that could affect repair durability.

In the future, tricuspid valve surgery will likely be replaced, at least in part, by transcatheter technologies.[56] While we investigated surgical annuloplasty in our current study, our findings likely translate well to transcatheter technologies.[9,37,41] For example, the Cardioband system (Edwards Lifesciences, Irvine, CA) and the Millipede IRIS System (Boston Scientific, Malborough, MA) are transcatheter technologies that will likely enter the US market soon. Their fundamental working principle does not significantly differ from DeVega suture annuloplasty. Therefore, the importance of our findings is not limited to surgical repair but also has an important implication to the future of tricuspid valve transcatheter technologies.

Limitations

Our study was naturally subjected to several limitations. Firstly, we performed this study in sheep and not in human patients. Therefore, extrapolating our observations to patients must be done with care. Furthermore, the sheep used in this study did not have tricuspid regurgitation. As such, leaflets from a diseased heart requiring surgical intervention may respond differently to DeVega suture annuloplasty. Additionally, it is important to note that we only analyzed the anterior leaflet and further studies would benefit from comparing the three leaflets of the tricuspid valve, especially because recent studies have noted microstructural and mechanical differences among leaflets.[34] Lastly, our study utilized sonomicrometry which is an invasive technology and may alter the *in-vivo* mechanics of the valve and its leaflets. Sonomicrometry crystals have a finite weight which may also affect the dynamics of the leaflets. Furthermore, we have simplified our analysis to only four crystals and two regions in the anterior leaflet, which cannot capture the previously reported heterogeneous behavior of tricuspid valve leaflets.[24]

CONCLUSION

In our current work, we provided the first evidence that cinching of the tricuspid valve annulus alters the mechanics of its anterior leaflet. Specifically, annular cinching reduced the leaflet's range of motion, reduced its opening and closing velocity, and reduced systolic strains. Especially, the latter finding is important as changes in tissue strain alter the leaflet's resident cells' mechanobiological equilibrium. Subsequently, such alterations may elicit an undesired maladaptive response that could contribute to the long-term failure of tricuspid annuloplasty. Our findings are important from a basic scientific perspective, but will additionally inform surgical guidelines on degree of cinching during annuloplasty.

ELECTRONIC SUPPLEMENTARY MATERIAL

The online version of this article (https://doi.org/10.1007/s10439-020-02586-x) contains supplementary material, which is available to authorized users.

ACKNOWLEDGMENTS

Partial support for this study through an internal grant from the Meijer Heart and Vascular Institute at Spectrum Health, from the American Heart Association (18CDA34120028), and the National Institutes of Health (F31HL145976) are very much appreciated.

CONFLICT OF INTEREST

Manuel K. Rausch has a speaking agreement with Edwards Lifesciences. None of the other authors have conflicts of interest to disclose.

REFERENCES

[1]Amini Khoiy, K., and R. Amini. On the biaxial mechanical response of porcine tricuspid valve leaflets. *J. Biomech. Eng*. 138(10):104504, 2016.
[2]Ayoub, S., G. Ferrari, R. C. Gorman, J. H. Gorman, F. J. Schoen, and M. S. Sacks. Heart valve biomechanics and underlying mechanobiology. *Comprehen. Physiol.* 6(4):1743–1780, 2016.
[3]Basu, A., and Z. He. Annulus tension on the tricuspid valve: an in-vitro study. *Cardiovasc. Eng. Technol.* 7(3):270–279, 2016.
[4]Beaudoin, J., W. E. Thai, B. Wai, M. D. Handschumacher, R. A. Levine, and Q. A. Truong. Assessment of mitral valve adaptation with gated cardiac computed tomography: validation with three-dimensional echocardiography

and mechanistic insight to functional mitral regurgitation. *Circulation* 6(5):784–789, 2013.

[5]Bishop, J. E., and G. Lindahl. Regulation of cardiovascular collagen synthesis by mechanical load. *Cardiovasc. Res*. 42(1):27–44, 1999.

[6]Bothe, W., E. Kuhl, J. P. E. Kvitting, M. K. Rausch, S. Goktepe, J. C. Swanson, S. Farahmandnia, N. B. Ingels, and D. C. Miller. Rigid, complete annuloplasty rings increase anterior mitral leaflet strains in the normal beating ovine heart. *Circulation* 124(11 SUPPL. 1):S81–S96, 2011.

[7]Bothe, W., J. P. E. Kvitting, M. K. Rausch, T. A. Timek, J. C. Swanson, D. H. Liang, M. Walther, E. Kuhl, N. B. Ingels, and D. C. Miller. Do annuloplasty rings designed to treat ischemic/functional mitral regurgitation alter left-ventricular dimensions in the acutely ischemic ovine heart? *J. Thorac. Cardiovasc. Surg*. 158(4):1058–1068, 2019.

[8]Chaput, M., M. D. Handschumacher, J. L. Guerrero, G. Holmvang, J. P. Dai-Bianco, S. Sullivan, G. J. Vlahakes, J. Hung, and R. A. Levine. Mitral leaflet adaptation to ventricular remodeling prospective changes in a model of ischemic mitral regurgitation. *Circulation* 120(SUPPL. 1):S99–S103, 2009.

[9]Curio, J., O. M. Demir, M. Pagnesi, A. Mangieri, F. Giannini, G. Weisz, and A. Latib. Update on the current landscape of transcatheter options for tricuspid regurgitation treatment. *Interven. Cardiol. Rev*. 14(2):54–61, 2019.

[10]Dal-Bianco, J. P., E. Aikawa, J. Bischoff, J. L. Guerrero, J. Hjortnaes, J. Beaudoin, C. Szymanski, P. E. Bartko, M. M. Seybolt, M. D. Handschumacher, S. Sullivan, M. L. Garcia, A. Mauskapf, J. S. Titus, J. Wylie-Sears, W. S. Irvin, M. Chaput, E. Messas, A. A. Hagege, A. Carpentier, and R. A. Levine. Myocardial infarction alters adaptation of the tethered mitral valve. *J. Am. Coll. Cardiol*. 67(3):275–287, 2016.

[11]Dal-Bianco, J. P., and R. A. Levine. The mitral valve is an actively adapting tissue: new imaging evidence. *Eur. Heart J. Cardiovasc. Imaging* 16(3):286–287, 2015.

[12]Dreyfus, G. D., R. P. Martin, K. M. J. Chan, F. Dulguerov, and C. Alexandrescu. Functional tricuspid regurgitation: a need to revise our understanding. *J. Am. Coll. Cardiol*. 65(21):2331–2336, 2015.

[13]Grande-Allen, K. J., J. E. Barber, K. M. Klatka, P. L. Houghtaling, I. Vesely, C. S. Moravec, and P. M. McCarthy. Mitral valve stiffening in end-stage heart failure: evidence of an organic contribution to functional mitral regurgitation. *J. Thorac. Cardiovasc. Surg*. 130(3):783–790, 2005.

[14]Grande-Allen, K. J., A. G. Borowski, R. W. Troughton, P. L. Houghtaling, N. R. Dipaola, C. S. Moravec, I. Vesely, and B. P. Griffin. Apparently normal mitral valves in patients with heart failure demonstrate biochemical and structural derangements: an extracellular matrix and echocardiographic study. *J. Am. Coll. Cardiol*. 45(1):54–61, 2005.

[15]Grande-Allen, K. J., and J. Liao. The heterogeneous biomechanics and mechanobiology of the mitral valve: implications for tissue engineering. *Curr. Cardiol. Rep*. 13(2):113–120, 2011.

[16]Holda, M. K., J. D. Zhingre Sanchez, M. G. Bateman, and P. A. Iaizzo. Right atrioventricular valve leaflet morphology redefined: implications for transcatheter repair procedures. *JACC Cardiovasc. Interven*. 12(2):169–178, 2019.

[17]Humphrey, J. D., E. R. Dufresne, and M. A. Schwartz. Mechanotransduction and extracellular matrix homeostasis. *Nat. Rev. Mol. Cell Biol*. 15(12):802–812, 2014.

[18]Jazwiec, T., M. Malinowski, H. Ferguson, J. Wodarek, N. Quay, J. Bush, M. Goehler, J. Parker, M. Rausch, and T. A.Timek. Effect of variable annular reduction on functional tricuspid regurgitation and right ventricular dynamics in an ovine model of tachycardia-induced cardiomyopathy. *J. Thorac. Cardiovasc. Surg*., 2020.

[19]Jensen, M. O., A. W. Siefert, I. Okafor, and A. P. Yoganathan. Measurement Technologies for Heart Valve Function. New York: Springer, pp. 115–149, 2018.

[20]Jett, S., D. Laurence, R. Kunkel, A. R. Babu, K. Kramer, R. Baumwart, R. Towner, Y. Wu, and C. H. Lee. An investigation of the anisotropic mechanical properties and anatomical structure of porcine atrioventricular heart valves. *J. Mech. Behav. Biomed. Mater*. 87:155–171, 2018.

[21]Khoiy, K., D. Biswas, T. N. Decker, K. T. Asgarian, F. Loth, and R. Amini. Surface strains of porcine tricuspid valve septal leaflets measured in ex vivo beating hearts. *J. Biomech. Eng*. 138(11):11100, 2016.

[22]Kong, F., T. Pham, C. Martin, R. McKay, C. Primiano, S. Hashim, S. Kodali, and W. Sun. Finite element analysis of tricuspid valve deformation from multi-slice computed tomography images. *Ann. Biomed. Eng*. 46(8):1112–1127, 2018.

[23]Laurence, D. W., E. L. Johnson, M. C. Hsu, R. Baumwart, A. Mir, H. M. Burkhart, G. A. Holzapfel, Y. Wu, and C. H. Lee. A pilot in silico modeling-based study of the pathological effects on the biomechanical function of tricuspid valves. *Int. J. Numer. Methods Biomed. Eng*., 2020.

[24]Laurence, D., C. Ross, S. Jett, C. Johns, A. Echols, R. Baumwart, R. Towner, J. Liao, P. Bajona, Y. Wu, and C. H. Lee. An investigation of regional variations in the biaxial mechanical properties and stress relaxation behaviors of porcine atrioventricular heart valve leaflets. *J. Biomech*. 83:16–27, 2019.

[25]Lee, C. H., D. W. Laurence, C. J. Ross, K. E. Kramer, A. R. Babu, E. L. Johnson, M. C. Hsu, A. Aggarwal, A. Mir, H. M. Burkhart, R. A. Towner, R. Baumwart, Y. Wu, C. H. Lee, D. W. Laurence, C. J. Ross, K. E. Kramer, A. R. Babu, E. L. Johnson, M. C. Hsu, A. Aggarwal, A. Mir, H. M. Burkhart, R. A. Towner, R. Baumwart, and Y. Wu. Mechanics of the tricuspid valve-from clinical diagnosis/treatment, in-vivo and in-vitro investigations, to patient-specific biomechanical modeling. *Bioengineering* 6(2):47, 2019.

[26]Lim, K. O. Mechanical properties and ultrastructure of normal human tricuspid valve chordae tendineae. *Jpn. J. Physiol*. 30(3):455–464, 1980.

[27]Malinowski, M., T. Jazwiec, M. Goehler, J. Bush, N. Quay, H. Ferguson, M. K. Rausch, and T. A. Timek. Impact of tricuspid annular size reduction on right ventricular function, geometry and strain. *Eur. J. Cardiothorac. Surg*. 56(2):400–408, 2019.

[28]Malinowski, M., T. Jazwiec, N. Quay, M. Goehler, M. K. Rausch, and T. A. Timek. The influence of tricuspid annuloplasty prostheses on ovine annular geometry and kinematics. *J. Thorac. Cardiovasc. Surg*. (2019).

[29]Malinowski, M., H. Schubert, J. Wodarek, H. Ferguson, L. Eberhart, D. Langholz, T. Jazwiec, M. K. Rausch, and T. A. Timek. Tricuspid annular geometry and strain after suture annuloplasty in acute ovine right heart failure. *Ann. Thorac. Surg*. 106(6):1804–1811, 2018.

[30]Mathur, M., M. Malinowski, T. A. Timek, and M. K. Rausch. Tricuspid annuloplasty rings: a quantitative comparison of size, non-planar shape, and stiffness. *Ann. Thorac. Surg*., 2020.

[31]Mathur, M., W. D. Meador, T. Jazwiec, M. Malinowski, T. A. Timek, and M. K. Rausch. The effect of downsizing on the normal tricuspid annulus. *Ann. Biomed. Eng*. 48(2):655–668, 2020.
[32]Meador, W. D., M. Malinowski, T. Jazwiec, M. Goehler, N. Quay, T. A. Timek, and M. K. Rausch. A fiduciary marker-based framework to assess heterogeneity and anisotropy of right ventricular epicardial strains in the beating ovine heart. *J. Biomech*. 80:179–185, 2018.
[33]Meador, W. D., M. Mathur, and M. K. Rausch. Tricuspid Valve Biomechanics: A Brief Review. New York: Springer, pp. 105–114, 2018.
[34]Meador, W. D., M. Mathur, G. P. Sugerman, T. Jazwiec, M. Malinowski, M. R. Bersi, T. A. Timek, and M. K. Rausch. A detailed mechanical and microstructural analysis of ovine tricuspid valve leaflets. *Acta Biomater*. 102:100–113, 2020.
[35]Misfeld, M., and H. H. Sievers. Heart valve macro- and microstructure. *Philos. Trans. R. Soc. B* 362(1484):1421–1436, 2007.
[36]Navia, J. L., E. R. Nowicki, E. H. Blackstone, N. A. Brozzi, D. E. Nento, F. A. Atik, J. Rajeswaran, A. M. Gillinov, L. G. Svensson, and B. W. Lytle. Surgical management of secondary tricuspid valve regurgitation: annulus, commissure, or leaflet procedure? *J. Thorac. Cardiovasc. Surg*. 139(6):1473–1482.e5, 2010.
[37]Oliveira, D. C., and C. G. Oliveira. The forgotten, not studied or not valorized tricuspid valve: the transcatheter revolution is coming. *Cardiol. Res*. 10(4):199–206, 2019.
[38]Pant, A. D., V. S. Thomas, A. L. Black, T. Verba, J. G. Lesicko, and R. Amini. Pressure-induced microstructural changes in porcine tricuspid valve leaflets. *Acta Biomater*. 67:248–258, 2018.
[39]Parolari, A., F. Barili, A. Pilozzi, and D. Pacini. Ring or suture annuloplasty for tricuspid regurgitation? A meta-analysis review. *Ann. Thorac. Surg*. 98:2255–2263, 2014.
[40]Pham, T., F. Sulejmani, E. Shin, D. Wang, and W. Sun. Quantification and comparison of the mechanical properties of four human cardiac valves. *Acta Biomater*. 54:345–355, 2017.
[41]Prendergast, B. D., H. Baumgartner, V. Delgado, O. Gerard, M. Haude, A. Himmelmann, B. Iung, M. Leafstedt, J. Lennartz, F. Maisano, E. A. Marinelli, T. Modine, M. Mueller, S. R. Redwood, O. Rorick, C. Sahyoun, E. Saillant, L. Sondergaard, M. Thoenes, K. Thomitzek, M. Tschernich, A. Vahanian, O. Wendler, E. J. Zemke, and J. J. Bax. Transcatheter heart valve interventions: where are we? Where are we going? *Eur. Heart J*. 40(5):422–440, 2019.
[42]Rausch, M. K. Growth and remodeling of atrioventricular heart valves: a potential target for pharmacological treatment? *Curr. Opin. Biomed. Eng*. 15:10–15, 2020.
[43]Rausch, M. K., W. Bothe, J. P. E. Kvitting, S. Goktepe, D. C. Miller, and E. Kuhl. In vivo dynamic strains of the ovine anterior mitral valve leaflet. *J. Biomech*. 44(6):1149–1157, 2011.
[44]Rausch, M. K., W. Bothe, J. P. E. Kvitting, J. C. Swanson, D. C. Miller, and E. Kuhl. Mitral valve annuloplasty: a quantitative clinical and mechanical comparison of different annuloplasty devices. *Ann. Biomed. Eng*. 40(3):750–761, 2012.
[45]Rausch, M. K., M. Malinowski, W. D. Meador, P. Wilton, A. Khaghani, and T. A. Timek. The effect of acute pulmonary hypertension on tricuspid annular height, strain, and curvature in sheep. *Cardiovasc. Eng. Technol*. 9(3):365–376, 2018.
[46]Rausch, M. K., M. Malinowski, P. Wilton, A. Khaghani, and T. A. Timek. Engineering analysis of tricuspid annular dynamics in the beating ovine heart. *Ann. Biomed. Eng*. 9(3):365–376, 2017.
[47]Rausch, M. K., F. A. Tibayan, D. Craig Miller, and E. Kuhl. Evidence of adaptive mitral leaflet growth. *J. Mech. Behav. Biomed. Mater*. 15:208–217, 2012.
[48]Rausch, M. K., F. A. Tibayan, N. B. Ingels, D. C. Miller, and E. Kuhl. Mechanics of the mitral annulus in chronic ischemic cardiomyopathy. *Ann. Biomed. Eng*. 41(10):2171–2180, 2013.
[49]Robitaille, M. C., R. Zareian, C. A. DiMarzio, K. Wan, and J. W. Ruberti. Small-angle light scattering to detect strain-directed collagen degradation in native tissue. *Interface Focus* 1(5):767–776, 2011.
[50]Ross, C. J., J. Zheng, L. Ma, Y. Wu, and C. H. Lee. Mechanics and microstructure of the atrioventricular heart valve chordae tendineae: a review. *Bioengineering* 7(1):1–15, 2020.
[51]Sacks, M. S., and A. P. Yoganathan. Heart valve function: a biomechanical perspective. *Philos. Trans. R. Soc. B* 362(1484):1369–1391, 2007.
[52]Shinn, S. H., V. Dayan, H. V. Schaff, J. A. Dearani, L. D. Joyce, B. Lahr, K. L. Greason, J. M. Stulak, and R. C. Daly. Outcomes of ring versus suture annuloplasty for tricuspid valve repair in patients undergoing mitral valve surgery. *J. Thorac. Cardiovasc. Surg*. 152(2):406–415.e3, 2016.
[53]Sielicka, A., E. L. Sarin, W. Shi, F. Sulejmani, D. Corporan, K. Kalra, V. H. Thourani, W. Sun, R. A. Guyton, and M. Padala. Pathological remodeling of mitral valve leaflets from unphysiologic leaflet mechanics after undersized mitral annuloplasty to repair ischemic mitral regurgitation. *J. Am. Heart Assoc*. 7(21):1–18, 2018.
[54]Silver, M. D., J. H. Lam, N. Ranganathan, and E. D. Wigle. Morphology of the human tricuspid valve. *Circulation* 43(3):333–348, 1971.
[55]Singh-Gryzbon, S., V. Sadri, M. Toma, E. L. Pierce, Z. A. Wei, and A. P. Yoganathan. Development of a computational method for simulating tricuspid valve dynamics. *Ann. Biomed. Eng*. 47(6):1422–1434, 2019.
[56]Singh-Gryzbon, S., A. W. Siefert, E. L. Pierce, and A. P. Yoganathan. Tricuspid valve annular mechanics: interactions with and implications for transcatheter devices. *Cardiovasc. Eng. Technol*. 10(2):193–204, 2019.
[57]Smith, K. J., M. Mathur, W. D. Meador, B. Phillips-Garcia, G. P. Sugerman, A. K. Menta, T. Jazwiec, M. Malinowski, T. A. Timek, and M. K. Rausch. Tricuspid chordae tendineae mechanics: insertion site, leaflet, and size-specific analysis and constitutive modelling. *Exper. Mech*., 2020.
[58]Spinner, E. M., D. Buice, C. H. Yap, and A. P. Yoganathan. The effects of a three-dimensional, saddle-shaped annulus on anterior and posterior leaflet stretch and regurgitation of the tricuspid valve. *Ann. Biomed. Eng*. 40(5):996–1005, 2012.
[59]Spinner, E. M., S. Lerakis, J. Higginson, M. Pernetz, S. Howell, E. Veledar, and A. P. Yoganathan. Correlates of tricuspid regurgitation as determined by 3D echocardiography: pulmonary arterial pressure, ventricle geometry, annular dilatation and papillary muscle displacement. *Circ. Cardiovasc. Imaging* 5(1):43–50, 2011.
[60]Stuge, O., and J. Liddicoat. Emerging opportunities for cardiac surgeons within structural heart disease. *J. Thorac. Cardiovasc. Surg*. 132(6):1258–1261, 2006.

[61]Suh, Y. J., B. C. Chang, D. J. Im, Y. J. Kim, Y. J. Hong, G. R. Hong, and Y. J. Kim. Assessment of mitral annuloplasty ring by cardiac computed tomography: Correlation with echocardiographic parameters and comparison between two different ring types. *J. Thorac. Cardiovasc. Surg*. 150(5):1082–1090, 2015.

[62]Timek, T. A., D. T. Lai, P. Dagum, D. Liang, G. T. Daughters, N. B. Ingels, and D. C. Miller. Mitral leaflet remodeling in dilated cardiomyopathy. *Circulation* 114(SUPPL. 1):518–523, 2006.

[63]Troxler, L. G., E. M. Spinner, and A. P. Yoganathan. Measurement of strut chordal forces of the tricuspid valve using miniature c ring transducers. *J. Biomech*. 45(6):1084–1091, 2012.